

Ground-based high spectral resolution observations of the entire terrestrial spectrum under extremely dry conditions

D. D. Turner,¹ E. J. Mlawer,² G. Bianchini,³ M. P. Cadetdu,⁴ S. Crewell,⁵ J. S. Delamere,² R. O. Knuteson,⁶ G. Maschwitz,⁵ M. Mlynzcak,⁷ S. Paine,⁸ L. Palchetti,³ and D. C. Tobin⁶

Received 28 February 2012; revised 13 April 2012; accepted 16 April 2012; published 16 May 2012.

[1] A field experiment was conducted in northern Chile at an altitude of 5.3 km to evaluate the accuracy of line-by-line radiative transfer models in regions of the spectrum that are typically opaque at sea level due to strong water vapor absorption. A suite of spectrally resolved radiance instruments collected simultaneous observations that, for the first time ever, spanned the entire terrestrial thermal spectrum (i.e., from 10 to 3000 cm^{-1} , or 1000 to 3.3 μm). These radiance observations, together with collocated water vapor and temperature profiles, are used to provide an initial evaluation of the accuracy of water vapor absorption in the far-infrared of two line-by-line radiative transfer models. These initial results suggest that the more recent of the two models is more accurate in the strongly absorbing water vapor pure rotation band. This result supports the validity of the Turner et al. (2012) study that demonstrated that the use of the more recent water vapor absorption model in climate simulations resulted in significant radiative and dynamical changes in the simulation relative to the older water vapor model. **Citation:** Turner, D. D., et al. (2012), Ground-based high spectral resolution observations of the entire terrestrial spectrum under extremely dry conditions, *Geophys. Res. Lett.*, 39, L10801, doi:10.1029/2012GL051542.

1. Introduction

[2] Accurate radiative transfer codes are required in order to represent gaseous absorption and other radiative processes in climate and weather prediction models, as well as in remote sensing algorithms. The most accurate radiative transfer codes treat the absorption by atmospheric gases in a line-by-line manner, using the spectral information provided by databases such as HITRAN [Rothman et al., 2009]. However, there are still significant uncertainties in line-by-

line radiative transfer models; these uncertainties are related to the line parameters in the spectral database (e.g., line absorption strengths and widths), the shape of the absorption line, and spectral features related to bimolecular (e.g., water vapor dimer) absorption. Because line-by-line modeling forms the basis for the approximations in less computationally-expensive band-models and correlated-k radiative transfer codes that are used in dynamical models, the spectroscopic uncertainties propagate into weather and climate simulations.

[3] The accuracy of line-by-line radiative transfer models is often evaluated using spectral radiative closure analysis, which require three components: (1) spectrally-resolved radiance observations; (2) characterization of the atmospheric state impacting these observations, such as profiles of water vapor, temperature, and cloud properties; and (3) a radiative transfer model that can be used to simulate the radiance measurements. Radiative closure exercises have successfully been used to evaluate and improve line-by-line radiative transfer models for many years [e.g., Serio et al., 2008; Turner et al., 2004; Tobin et al., 1999]. However, adequate evaluation using ground-based observations requires that the atmospheric transmissivity be significantly larger than zero (i.e., >5%).

[4] In particular, evaluation of water vapor absorption parameters, both associated with absorption lines and water vapor continuum absorption, is very difficult to make in strongly absorbing water vapor bands due to the opacity of the atmosphere. Therefore, it is essential that radiative closure studies targeting these spectral regions are based on surface spectral measurements from locations characterized by very low abundances of precipitable water vapor (PWV). The Atmospheric Radiation Measurement (ARM) program conducted two such field experiments: the first and second Radiative Heating in Underexplored Bands Campaigns (RHUBC) [Turner and Mlawer, 2010]. RHUBC-I occurred at the ARM North Slope of Alaska site (71.3°N, 97.4°W, 8 m MSL) in 2007, while RHUBC-II was held at an altitude of 5.3 km in the Atacama Desert in northern Chile (23.0°S, 67.8°W). The PWV at this latter site can go as low as 0.2 mm, which is nearly 20× smaller than typical mid-latitude sites. At these small amounts of PWV, large portions of the electromagnetic spectrum, including regions of the water vapor pure rotation band (from 0 to approximately 625 cm^{-1}) become semitransparent, allowing the spectroscopic foundation of radiative transfer calculations to be evaluated.

[5] Previous campaigns similar to RHUBC-II have yielded valuable results. Measurements made in the 300–600 cm^{-1} range during RHUBC-I and ECOWAR [Serio et al., 2008], as well as observations at 5 cm^{-1} during a separate field experiment [Turner et al., 2009; Payne et al., 2011], led to sizeable modifications to the previously derived strength of the water vapor continuum in the 10–700 cm^{-1} region

¹National Severe Storms Laboratory, NOAA, Norman, Oklahoma, USA.

²Atmospheric and Environmental Research, Inc., Lexington, Massachusetts, USA.

³Istituto di Fisica Applicata “Nello Carrara,” Consiglio Nazionale delle Ricerche, Sesto Fiorentino, Italy.

⁴Argonne National Laboratory, Argonne, Illinois, USA.

⁵Institut für Geophysik und Meteorologie, University of Cologne, Cologne, Germany.

⁶Space Science and Engineering Center, University of Wisconsin-Madison, Madison, Wisconsin, USA.

⁷NASA Langley Research Center, Hampton, Virginia, USA.

⁸Smithsonian Astrophysical Observatory, Cambridge, Massachusetts, USA.

Corresponding author: D. Turner, National Severe Storms Laboratory, NOAA, 120 David L. Boren Blvd., Norman, OK 73072, USA. (dave.turner@noaa.gov)

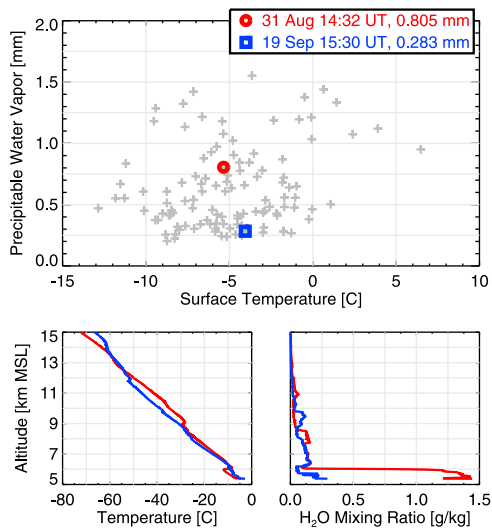


Figure 1. (top) Radiosonde observations of surface temperature and PWV during RHUBC-II, including those for the ‘wet’ (red) and ‘dry’ (blue) case studies, and (bottom) the temperature and water vapor mixing ratio profiles for the two case studies.

[Delamere *et al.*, 2010]. This change was implemented into the radiation code utilized by the Community Earth System Model (CESM) and evaluated relative to the baseline CESM. The analysis of the two climate model simulations indicated that this change in the water vapor absorption strength in the model had a statistically significant impact on both the radiation and dynamics [Turner *et al.*, 2012] with changes in the vertical structure of temperature, humidity, and cloud amount, all of which impacted the diabatic heating profile. This study highlighted the importance of properly modeling the nature of water vapor absorption in strongly absorbing water vapor bands.

[6] RHUBC-II included instruments that, for the first time, collected spectrally resolved radiance observations over the entire terrestrial spectrum. Examples of these observations are provided here, including an initial evaluation of two versions of the often-used line-by-line model LBLRTM [Clough *et al.*, 2005; Mlawer *et al.*, 2012] in spectral regions that are typically opaque. Data from this experiment will allow the evaluation of the modeled strength of the water vapor absorption in the middle of the far-infrared portion of the spectrum ($20\text{--}300\text{ cm}^{-1}$), a spectral region that has not been evaluated before. The scientific motivation and details of the RHUBC-II experiment, including a full list of

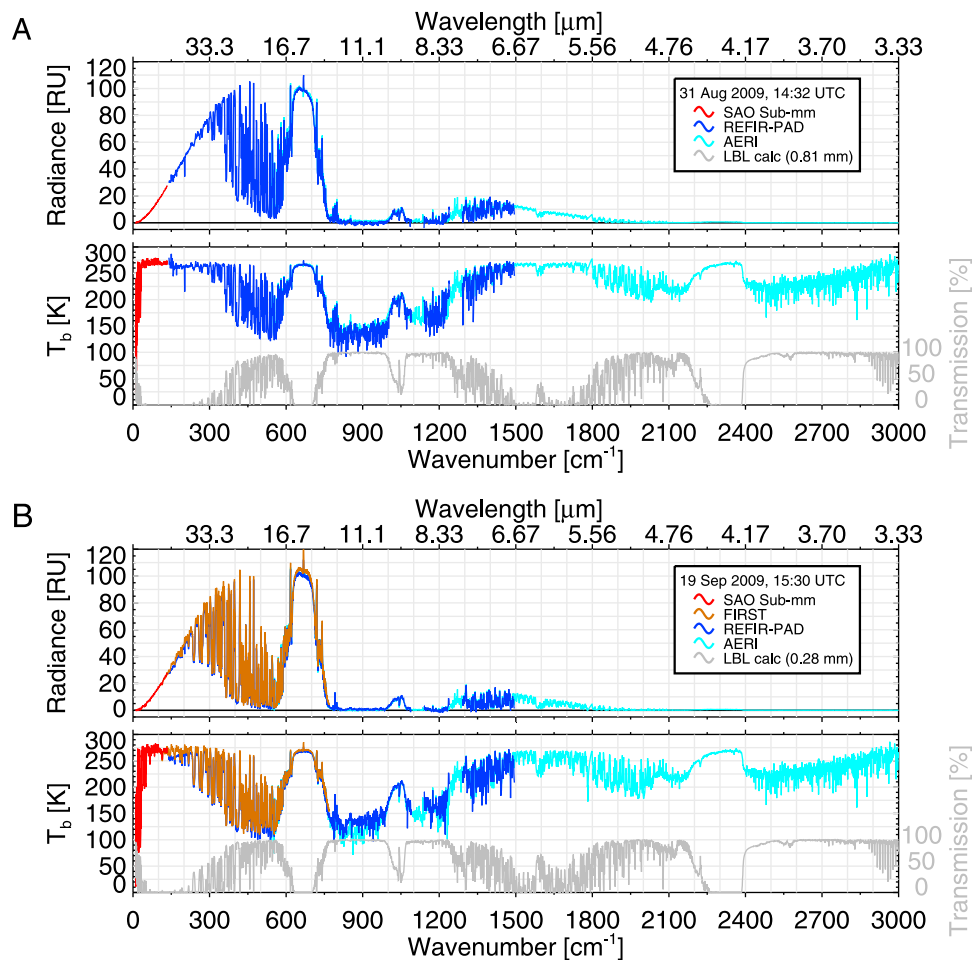


Figure 2. The observed downwelling radiance and brightness temperature over the entire terrestrial thermal spectrum observed during the (a) wet and (b) dry case during RHUBC-II. The gray spectra are the atmospheric transmittance spectra computed from the LBLRTM (axis on right). A radiance unit (RU) is $1\text{ mW} / (\text{m}^2\text{ sr cm}^{-1})$.

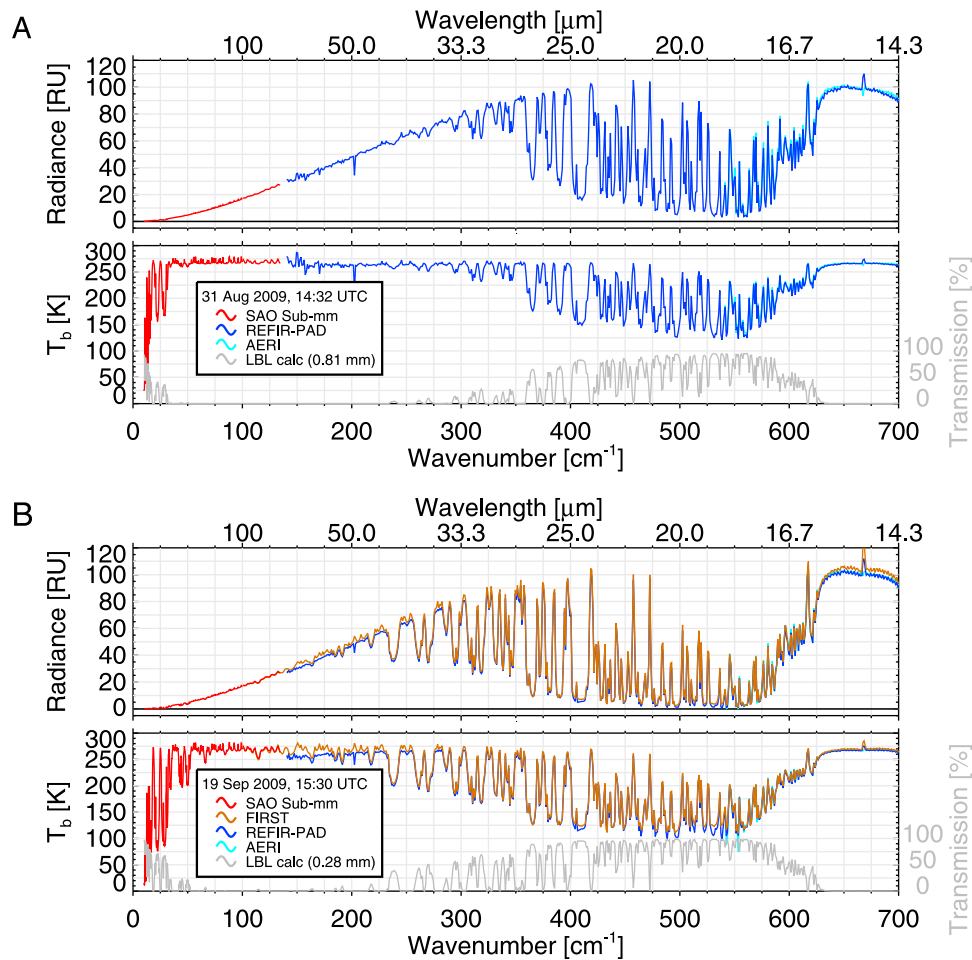


Figure 3. Same as Figure 2, but only over the water vapor pure rotation band in the far-infrared.

instruments that were deployed, is provided in *Turner and Mlawer* [2010].

2. Data

[7] Four Fourier Transform Spectrometers (FTS) instruments made measurements of the terrestrial infrared spectrum during RHUBC-II:

[8] 1. The Atmospheric Emitted Radiance Interferometer (AERI) measures radiance between 520–3000 cm^{-1} . Liquid nitrogen (LN_2) was used to cool the detectors to ~ 75 K. It is calibrated by two high-emissivity blackbodies, and after accounting for the non-linearity of the detector, has a radiometric accuracy better than 1% of the ambient radiance ($3\text{-}\sigma$) [*Knuteson et al.*, 2004].

[9] 2. The Far Infrared Spectroscopy of the Troposphere (FIRST) is a compact plane FTS that has sensitivity from 100–1600 cm^{-1} . The detector is cooled by liquid helium (LHe) to ~ 4 K to reduce instrument noise. The FIRST beamsplitter has absorption features at wavenumbers larger than 780 cm^{-1} , and thus only data at smaller wavenumbers are used in this study. Additional details on the FIRST design and calibration are provided in *Mlynczak et al.* [2006].

[10] 3. The Radiation Explorer in the Far Infrared – Prototype for Applications and Development (REFIR-PAD) utilizes pyroelectric detectors operating at 25°C and is able to sense radiation from 100–1400 cm^{-1} [*Palchetti et al.*, 2005]. The

REFIR-PAD beamsplitter has some absorption features around 1110 and 1250 cm^{-1} ; data in these spectral regions aren't analyzed here. Like the AERI, both the FIRST and REFIR-PAD use two blackbodies at hot and near ambient temperatures for calibration.

[11] 4. The Smithsonian Astrophysical Observatory (SAO) sub-mm FTS is a step-scanned interferometer using polarization chopping between a scene and reference target. A balanced pair of bolometers, cooled to 4 K with LHe, detects the modulated signal [*Paine et al.*, 2000]. The FTS viewed a LN_2 target on each operation day, and an ambient temperature dependent calibration was derived. The spectral range observed by this instrument is 10–115 cm^{-1} . The field-of-view of the SAO FTS, as well as the AERI, FIRST, and REFIR-PAD, is less than 2 degrees.

[12] Also in operation at the site were two instruments that made measurements in the microwave region. The G-band water vapor radiometer profiler (GVRP) [*Cimini et al.*, 2009] uses a single frequency-agile synthesizer to measure emission in 15 channels from 170 to 183.31 GHz (5.6–6.1 cm^{-1}), while the Humidity and Temperature Profiler (HATPRO) [*Rose et al.*, 2005] uses direct detection to measure emission in 7 channels from 22–31 GHz (0.74–1.03 cm^{-1}) and 7 channels from 51–58 GHz (1.7–1.9 cm^{-1}). Both radiometers were calibrated with LN_2 and tip curves [*Han and Westwater*, 2000], depending on channel opacity.

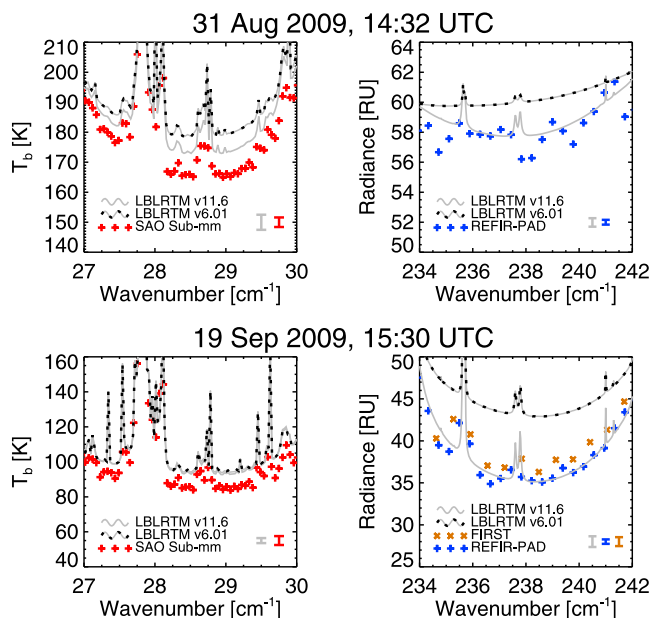


Figure 4. Comparison of monochromatic LBLRTM calculations for the (top) wet and (bottom) dry cases in (left and right) two microwindows. The calculations were performed using two different versions of the model. Data from the SAO sub-mm, FIRST, and REFIR are shown with symbols. In the lower right-hand corner of each panel are error bars ($1-\sigma$) at 29 and 238 cm^{-1} ; the calculation uncertainty is associated with $\pm 3\%$ error in PWV. The transmission of the atmosphere at 29 and 238 cm^{-1} , computed using LBLRTM v11.6, is 35% and 5% on 31 Aug and 70% and 40% on 19 Sep.

[13] Operations were conducted on about 40 days during the 3-month experiment. Vaisala RS92-k radiosondes were launched during periods when the sky conditions were clear or cirrus; typically 1–4 sondes were launched per day. The range of surface temperatures and PWV observed by the ~ 120 radiosondes that ascended to at least 15 km is shown in Figure 1. The radiosonde-observed humidity profiles have been scaled to agree with the downwelling measurements from the GVRP; the accuracy of the resulting PWV values is estimated to be $\pm 3\%$ [Cimini *et al.*, 2009]. Previous radiative closure exercises have scaled the humidity profile from Vaisala radiosondes to agree with microwave radiometer observations in order to reduce the uncertainty in the sonde observations [e.g., Turner *et al.*, 2004; Cady-Pereira *et al.*, 2008].

3. Results

[14] Two clear sky cases with differing PWV amounts were selected from the dataset to illustrate the spectral coverage and utility of the data. The collocated micropulse lidar was not functioning during most of the experiment, and thus clear skies were determined from manual sky observations and the lack of temporal variability in the downwelling infrared spectra in transparent channels (e.g., at 900 cm^{-1}). The two cases are on 31 Aug with a PWV of 0.81 mm and 19 Sep with a PWV of 0.28 mm; both cases have similar surface temperatures (Figure 1).

[15] Figure 2 shows the radiance observations from the AERI, FIRST, REFIR-PAD and SAO sub-mm over the

entire terrestrial spectrum in both radiance and brightness temperature (T_b). The gray spectrum is the atmospheric transmission computed with the LBLRTM radiative transfer code. These are, to our knowledge, these are the first surface-based spectrally resolved radiance measurements that span the entire terrestrial spectrum from 3 to over 1000 μm .

[16] Figure 3 shows the downwelling radiance in the strongly absorbing water vapor rotation band. The RHUBC-II observations capture the “opening” (i.e., semi-transparency) of the microwindows on both the long- and short-wavenumber side of this absorption band, and illustrate the uniqueness of the RHUBC-II dataset for studies to evaluate the accuracy of radiative transfer models in this spectral region.

[17] Figure 4 illustrates two microwindows, one on either side of the region of peak absorption of the water vapor rotation band, that were observed during RHUBC-II. Monochromatic line-by-line downwelling radiance calculations were made with two versions of the LBLRTM (see Table 1 for model details). For these cases, the change in PWV from the original RS92 radiosonde based on the GVRP measurements were 7.7% and 2.5% in the wet and dry case, respectively. The error bars (lower right-hand corner of each panel of Figure 4) illustrate, for 29 and 239 cm^{-1} , the uncertainty in the observations and the calculations, where the latter assume a $\pm 3\%$ uncertainty in PWV. This figure illustrates that for these cases the observations in these two microwindows are better fit by the LBLRTM v11.6. At 239 cm^{-1} , the superior results of the more recent model are likely due to an improved water vapor continuum, which was formulated taking into account the results from RHUBC-I. Interpretation of the results at 29 cm^{-1} is complicated by the multiple refinements that have been applied to the continuum model since CKD_v2.4/LBLRTM_v6.01, including a $\sim 35\%$ increase in the nitrogen continuum based on Boissoles *et al.* [2003] and a decrease in water vapor foreign continuum absorption. These changes more-or-less cancel out for the dry case, but for the wet case the overall effect is decreased absorption in the more recent model. These two cases suggest that the absorption in this region may need to be reduced to obtain better agreement with observations, but analysis of the full RHUBC-II dataset will be necessary to substantiate this result and determine if any deficiency lies in the water vapor continuum or in another component of the model.

[18] Many GCMs use the water vapor continuum absorption model embodied in LBLRTM v6.01. These results, together with the GCM simulation study by Turner *et al.* [2012], suggest that an improvement in modeling can be realized by updating the water vapor continuum model to the latest version.

4. Summary

[19] The RHUBC-II experiment collected, for the first time, spectrally resolved measurements across the entire thermal terrestrial spectrum, and specifically across the entire water vapor pure rotation band. The unique spectral

Table 1. LBLRTM Model Configuration

LBLRTM Version	Line Parameter Database	Continuum Version
v6.01	aer_hitran2000 update 1.1	CKD v2.4
v11.6	aer_v2.2 (based on HITRAN 2004)	MT_CKD v2.4

observations, together with the additional instruments that characterized the atmospheric state (e.g., radiosondes, GVRP, HATPRO) are being used to evaluate gaseous absorption models in spectral regions that have significant uncertainty due to lack of observational data. One advantage to downwelling ground-based spectral observations collected during RHUBC-II, as opposed to satellite-borne observations (that currently don't exist in the far-infrared), is that the cold background results in a larger signal from the continuum than an upwelling radiance observation that includes emission from the earth's surface.

[20] A full analysis of the RHUBC-II dataset that uses all of the available cases and accounts for details ignored here, such as instrument filter functions and potential small contributions within the instruments (i.e., the so-called chimney effect, which impacts the radiance slightly in the opaque elements of the spectrum), is currently underway. This future study will consider the colder and wetter cases observed during previous related field experiments such as RHUBC-I and ECOWAR, thereby allowing challenging issues such as the temperature dependence of the water vapor continuum absorption to be investigated with atmospheric observations. The resulting improvement to line-by-line radiative transfer models, and the subsequent improvement of the radiative transfer models in GCMs, will improve the community's ability to simulate climate.

[21] **Acknowledgments.** The RHUBC-II campaign was organized as part of the U.S. Department of Energy's Atmospheric Radiation Measurement (ARM) program, which is sponsored by the Office of Science, Office of Biological and Environmental Research, Climate and Environmental Sciences Division. RHUBC-II was also supported in part by NASA, the Italian National Research Council, the Smithsonian Institution, and the German Science Foundation (DFG). We would like to thank the many scientists and engineers who helped make the collection of this dataset possible, including Alex Carrizo and operations staff at AstroNorte, Kim Nitschke, Jim Mather, Charles Brinkmann, Troy Culgan, Mike Ryzcek, Rich Cageao, Glenn Farnsworth, Mike Wojcik, Jason Swasey, Joe Lee, Erik Syrstad, Dave Johnson, Julio Marin, Arlette Chacon, Toufic Hawat, Huabai Li, Marcos Diaz, Francesco Castagnoli, Denny Hackel, Ray Garcia, Hank Revercomb, Rich Coulter, and Tim Wagner. Additional information on the RHUBC-II experiment can be found at <http://acrif-campaign.arm.gov/rhubc/>. RHUBC-II data are available from the ARM data archive as an IOP dataset at <http://www.archive.arm.gov>.

[22] The Editor thanks the two anonymous reviewers for assisting with the evaluation of this paper.

References

- Boissoles, J., C. Boulet, R. H. Tipping, A. Brown, and Q. Ma (2003), Theoretical calculations of the translation-rotation collision-induced absorption in N₂-N₂, O₂-O₂ and N₂-O₂ Pairs, *J. Quant. Spectrosc. Radiat. Transfer*, *82*, 505–516, doi:10.1016/S0022-4073(03)00174-2.
- Cady-Pereira, K. E., M. W. Shephard, D. D. Turner, E. J. Mlawer, S. A. Clough, and T. J. Wagner (2008), Improved daytime column-integrated precipitable water vapor from Vaisala radiosonde humidity sensors, *J. Atmos. Oceanic Technol.*, *25*, 873–883, doi:10.1175/2007JTECHA1027.1.
- Cimini, D., F. Nasir, E. R. Westwater, V. H. Payne, D. D. Turner, E. J. Mlawer, M. L. Exner, and M. P. Cadetdu (2009), Comparisons of ground-based millimeter-wave observations and simulations in the Arctic winter, *IEEE Trans. Geosci. Remote Sens.*, *47*, 3098–3106, doi:10.1109/TGRS.2009.2020743.
- Clough, S. A., M. W. Shephard, E. J. Mlawer, J. S. Delamere, M. J. Iacono, K. Cady-Pereira, S. Boukabara, and P. D. Brown (2005), Atmospheric radiative transfer modeling: A summary of the AER codes, *J. Quant. Spectrosc. Radiat. Transfer*, *91*, 233–244, doi:10.1016/j.jqsrt.2004.05.058.
- Delamere, J. S., S. A. Clough, V. Payne, E. J. Mlawer, D. D. Turner, and R. Gamache (2010), A far-infrared radiative closure study in the Arctic: Application to water vapor, *J. Geophys. Res.*, *115*, D17106, doi:10.1029/2009JD012968.
- Han, Y., and E. R. Westwater (2000), Analysis and improvement of tipping calibration for ground-based microwave radiometers, *IEEE Trans. Geosci. Remote Sens.*, *38*, 1260–1276, doi:10.1109/36.843018.
- Knuteson, R. O., et al. (2004), The Atmospheric Emitted Radiance Interferometer: Part II. Instrument performance, *J. Atmos. Oceanic Technol.*, *21*, 1777–1789, doi:10.1175/JTECH-1663.1.
- Mlawer, E. J., V. H. Payne, J.-L. Moncet, J. S. Delamere, M. J. Alvarado, and D. C. Tobin (2012), Development and recent evaluation of the MT_CKD model of continuum absorption, *Philos. Trans. R. Soc. A*, in press.
- Mlyneczek, M. G., D. G. Johnson, H. Latvakoski, K. Jucks, M. Watson, G. Bingham, D. P. Kratz, W. A. Traub, S. J. Wellard, and C. R. Hyde (2006), First light from the far-infrared spectroscopy of the troposphere (FIRST) instrument, *Geophys. Res. Lett.*, *33*, L07704, doi:10.1029/2005GL025114.
- Paine, S., R. Blundell, D. C. Papa, J. W. Barrett, and S. J. E. Radford (2000), A Fourier transform spectrometer for measurement of atmospheric transmission at submillimeter wavelengths, *Publ. Astron. Soc. Pac.*, *112*, 108–118, doi:10.1086/316497.
- Palchetti, L., G. Bianchini, F. Castagnoli, B. Carli, C. Serio, F. Esposito, V. Cuomo, R. Rizzi, and T. Maestri (2005), Breadboard of the Fourier transform spectrometer for the Radiation Explorer in the Far Infrared (REFIR) atmospheric mission, *Appl. Opt.*, *44*, 2870–2878, doi:10.1364/AO.44.002870.
- Payne, V. H., E. J. Mlawer, K. E. Cady-Pereira, and J.-L. Moncet (2011), Water vapor continuum absorption in the microwave, *IEEE Trans. Geosci. Remote Sens.*, *49*, 2194–2208, doi:10.1109/TGRS.2010.2091416.
- Rose, T., S. Crewell, U. Löhnert, and C. Simmer (2005), A network suitable microwave radiometer for operational monitoring of the cloudy atmosphere, *Atmos. Res.*, *75*, 183–200, doi:10.1016/j.atmosres.2004.12.005.
- Rothman, L. S., et al. (2009), The HITRAN 2008 spectroscopic database, *J. Quant. Spectrosc. Radiat. Transfer*, *110*, 533–572, doi:10.1016/j.jqsrt.2009.02.013.
- Serio, C., et al. (2008), Retrieval of foreign-broadened water vapor continuum coefficients from emitted spectral radiance in the H₂O rotational band from 240–590 cm⁻¹, *Opt. Express*, *16*, 15,816–15,833, doi:10.1364/OE.16.015816.
- Tobin, D. C., et al. (1999), Downwelling spectral radiance observations at the SHEBA ice station: Water vapor continuum measurements from 17 to 26 μm, *J. Geophys. Res.*, *104*, 2081–2092, doi:10.1029/1998JD200057.
- Turner, D. D., and E. J. Mlawer (2010), Radiative heating in underexplored bands campaigns (RHUBC), *Bull. Am. Meteorol. Soc.*, *91*, 911–923, doi:10.1175/2010BAMS2904.1.
- Turner, D. D., et al. (2004), The QME AERI LBLRTM: A closure experiment for downwelling high spectral resolution infrared radiance, *J. Atmos. Sci.*, *61*, 2657–2675, doi:10.1175/JAS3300.1.
- Turner, D. D., U. Löhnert, M. Cadetdu, S. Crewell, and A. Vogelmann (2009), Modifications to the water vapor continuum in the microwave suggested by ground-based 150 GHz observations, *IEEE Trans. Geosci. Remote Sens.*, *47*, 3326–3337, doi:10.1109/TGRS.2009.2022262.
- Turner, D. D., A. Merrelli, D. Vimont, and E. J. Mlawer (2012), Impact of modifying the longwave water vapor continuum absorption model on Community Earth System Model simulations, *J. Geophys. Res.*, *117*, D04106, doi:10.1029/2011JD016440.